



## Supplementary Materials

# Improving Photocatalytic Stille Coupling Reaction by CuPd Alloy-Doped Ordered Mesoporous TiO<sub>2</sub>

Ting Tang <sup>1</sup>, Lehong Jin <sup>1</sup>, Wei Chai <sup>2</sup>, Jing Shen <sup>3</sup>, Zhenmin Xu <sup>3,\*</sup> and Haifang Mao <sup>3,\*</sup><sup>1</sup> School of Public Health, Hangzhou Normal University, Hangzhou 311121, China<sup>2</sup> Department of Chemical Engineering, Zaozhuang Vocational College, Zaozhuang 277800, China<sup>3</sup> School of Chemical and Environmental Engineering, Shanghai Institute of Technology, Shanghai 201418, China

\* Correspondence: zhenminxufy@163.com (Z.X.); mhf@sit.edu.cn (H.M.)

**Characterization.** The crystal structure was recorded using X-ray diffraction (XRD, Rigaku Dmax-3C Cu-Kα). The morphology was observed using transmission electron microscopy (TEM, JEOL-2010F, 200 KV) and field emission scanning electron microscopy (FESEM, HITACHI S4800). The UV–Vis diffuse reflectance spectra (DRS) were obtained on a UV-vis spectrophotometer (UV-Vis DRS, Shimadzu UV-2450). The Brunauer–Emmett–Teller (BET) method was used to calculate specific surface area (SBET), and the Barrett–Joyner–Halenda (BJH) model was used to calculate pore volume (VP) and pore diameter (DP). Surface electronic states were determined using X-ray photoelectron spectroscopy (XPS, PHI 5000 Versaprobe II). The shift in the binding energy due to relative surface charging was corrected using the C1S level at 284.8 eV as an internal standard. The CuPd loading was determined using an inductively coupled plasma optical emission spectrometer (ICP-OES, Varian VISTAMPX). The Fourier transform infrared spectra (FT-IR) were obtained using an AVATAR 370 FT-IR spectrometer. The photoelectrochemical measurements were carried out using a conventional three-electrode, single-compartment quartz cell on an electrochemical station (CHI 660D). A bias voltage of 0.5 V was used to drive the transfer of photogenerated electrons from the working electrode to the platinum electrode. A Na<sub>2</sub>SO<sub>4</sub> aqueous solution (0.50 mol/L) was used as the electrolyte. A 300 W Xe lamp with a UV filter ( $\lambda > 420$  nm) was used as the visible light source; this was positioned 10 cm away from the photoelectrochemical cell. Electrochemical Impedance Spectroscopy (EIS) tests were carried out at the bias voltage of 0.3 V and recorded over a frequency range of  $0.01^{-1} \times 10^5$  Hz with the amplitude of 5 mV.

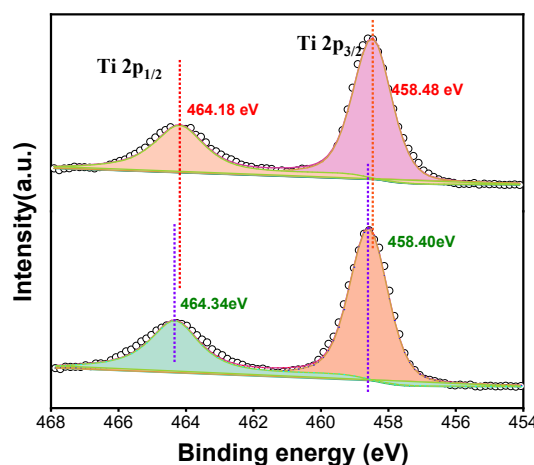
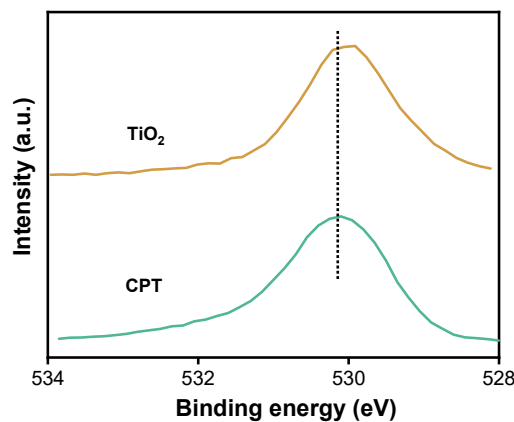
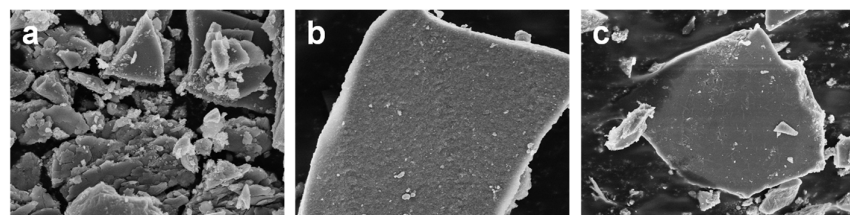


Figure S1. Ti 2p XPS spectra of CPT-1.5.



**Figure S2.** O 2p XPS spectra of CPT-1.5.



**Figure S3.** FESEM images of (a) CPT-0.2, (b) CPT-1.5, and (c) CPT-2.0.

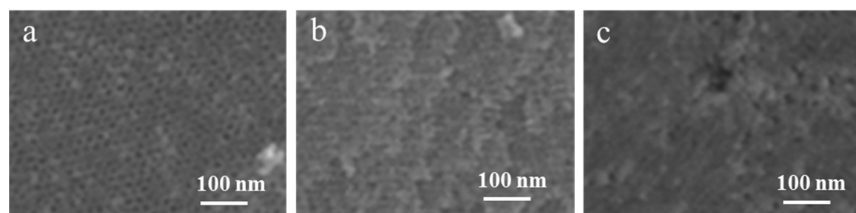


**Figure S4.** High-resolution FESEM images of (a) CPT-0.2, (b) CPT-1.5, and (c) CPT-2.0.

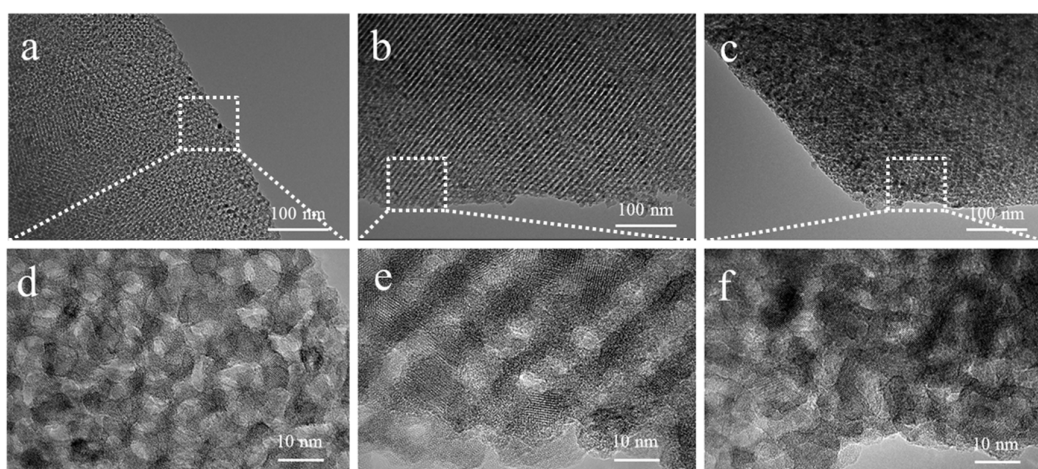


**Figure S5.** High-resolution TEM images of (a,d) CPT-0.2, (b,e) CPT-1.0, and (c,f) CPT-2.0.

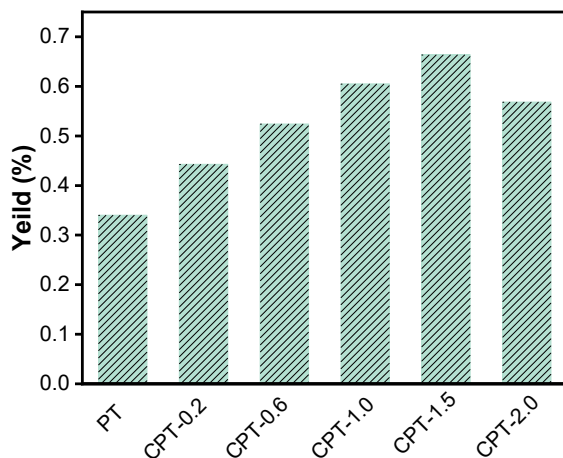


**Figure S6.** The yield of styrene during the photocatalytic Stille reaction of Iodobenzene and Tributyl(vinyl)tin in different samples.

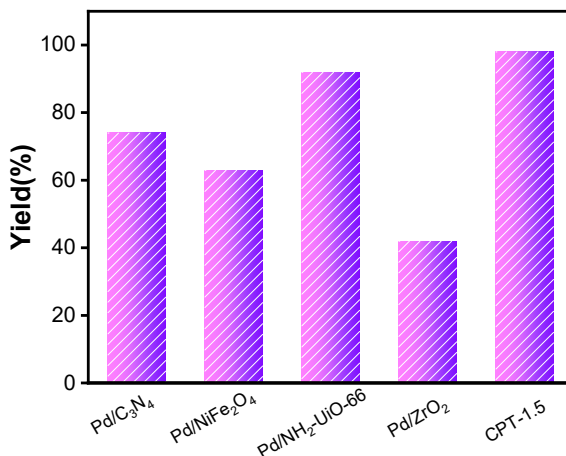


**Figure S7.** Comparison of the activity of CPT-1.5 with those previously reported for other photocatalysts during photocatalytic Stille reaction.

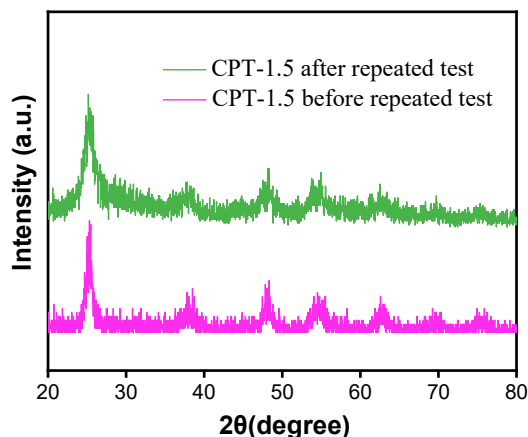


**Figure S8.** XRD of CPT-1.5 before and after repeated test in photocatalytic Stille reaction.

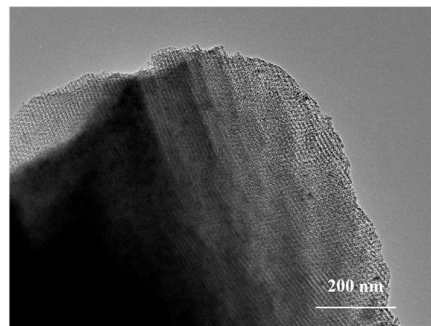


Figure S9. TEM of CPT-1.5 after repeated test in photocatalytic Stille reaction.

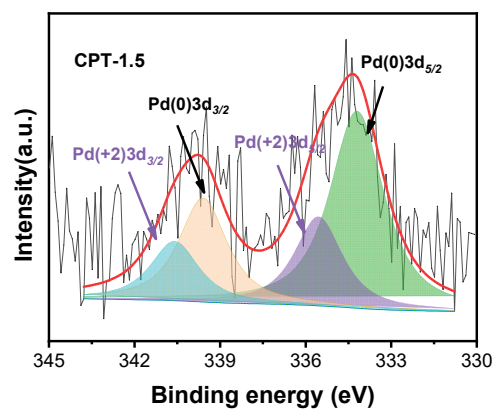


Figure S10. Pd 3d XPS spectra of CPT-1.5 after repeated test in photocatalytic Stille reaction.

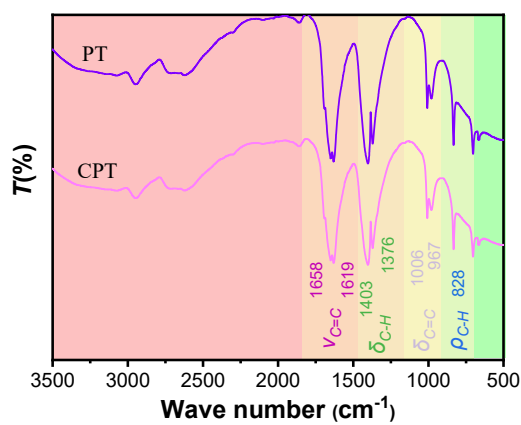
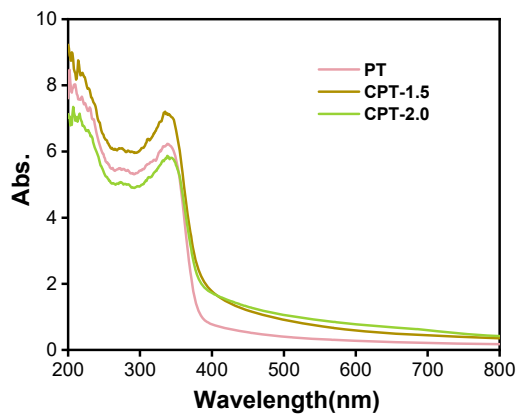
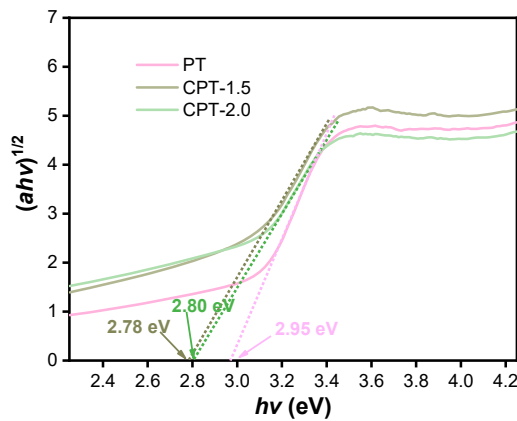


Figure S11. FT-IR of tributyl(vinyl)tin in different catalysts during photocatalytic Stille reaction.



**Figure S12.** UV-Vis DRS of PT, CPT-1.5, and CPT-2.0.



**Figure S13.** The plots of transformed Kubelka–Munk function versus the energy of light.

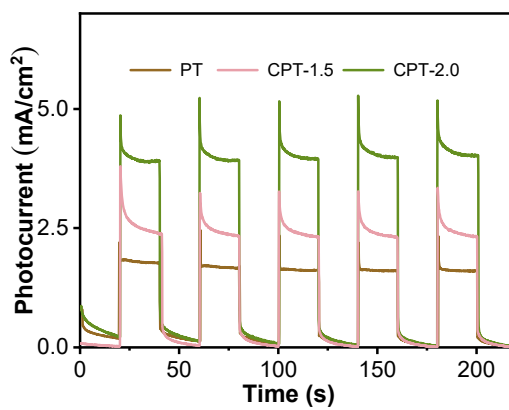


**Figure S14.** Transient photocurrent responses of PT, CPT-1.5, and CPT-2.0.

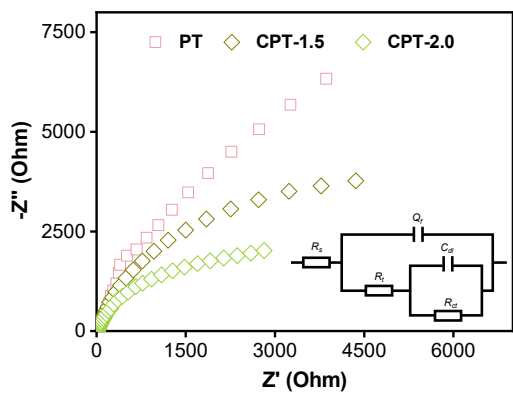


**Figure S15.** EIS Nyquist plots of PT, CPT-1.5, and CPT-2.0.

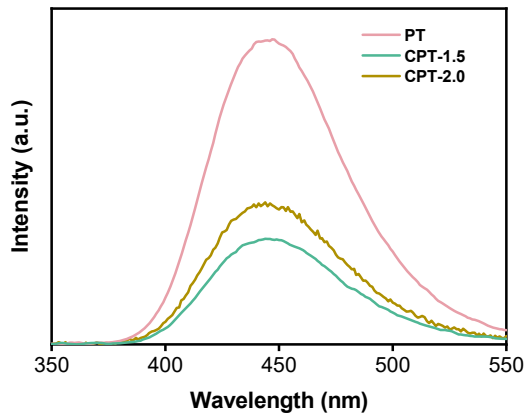


**Figure S16.** PL curves of PT, CPT-1.5, and CPT-2.0.

**Table S1.** Structural parameters of different samples.

<b>Sample</b>	<b>S<sub>BET</sub> (m<sup>2</sup>/g)</b>	<b>V<sub>p</sub> (cm<sup>3</sup>/g)</b>	<b>D<sub>p</sub> (nm)</b>
CPT-0.2	180	0.46	4.1
CPT-1.5	164	0.32	3.8
CPT-2.0	155	0.30	3.2

**Table S2.** Content of CuPd in different samples.

<b>Sample</b>	<b>ICP</b>		<b>XPS</b>	
	<b>Pd</b>	<b>Cu</b>	<b>Pd</b>	<b>Cu</b>
CPT-0.2	0.72	0.14	0.62	0.12
CPT-0.6	0.67	0.34	0.61	0.28
CPT-1.0	0.63	0.74	0.58	0.64
CPT-1.5	0.69	1.23	0.62	1.11
CPT-2.0	0.66	1.58	0.54	1.32